

THE INFLUENCE OF THE ELECTROMAGNETIC FIELD ON THE SURFACE HARDENING PROCESS OF FLAT WORKPIECES

Livia Bandici[1], D. Ţelea[2], T. Leuca[3], Şt. Nagy[1], D. Trip[4], A. Burcă[4]
[1]University of Oradea, Faculty of Electrical Engineering and Information Technology, Department of Electrical Engineering, Postal address1, 1 Universitatii Street, 410087 Oradea, Romania, e-mail: lbandici@uoradea.ro
[2]S.C. Tecor S.A. Oradea, e-mail: darius@tecor.ro
[3] University of Oradea, Faculty of Electrical Engineering and Information Technology, Department of Electrical Engineering, Academy of Romanian Scientists, Romania, e-mail: tleuca@uoradea.ro
4 University of Oradea, Faculty of Electrical Engineering and Information Technology, Department of Electronics and Telecommunications, Romania, e-mail: dtrip@uoradea.ro; aburca@uoradea.ro/

ABSTRACT: This paper presents the results obtained by numerical modelling of the surface induction hardening process of a workpiece. We performed numerical modelling by using the ELTA program. In this study, we aimed to establish the electrical parameters in order to optimize the surface hardening process.

KEYWORDS: electromagnetic field, modelling, surface hardening.

1. INTRODUCTION

James C. Maxwell was the one who combined electrical and magnetic phenomena, transposing them into mathematical equations [1]. These equations underlie the solving of problems related to the penetration of the electromagnetic field into conductive environments.

With the emergence of high performance computers, analytical methods are no longer so often used, but analytical calculation results are very useful for selecting the initial process parameters (time, power, frequency) [2].

Surface hardening heat treatment is one of the most important applications of induction heating. This process concentrates a large amount of energy in a layer in which the higher the frequency the lower the thickness is [3], [4]. Using high frequencies ensures high power density and fast heat concentration in a well-located region. At the end of the hardening process in that region, the metallurgical structure will be changed, but the properties of the material are not affected.

2. ELECTROMAGNETIC FIELD ANALYSIS IN A SINUSOIDAL QUASY-STATIONARY REGIME

The analysis of the surface hardening process is particularly complicated, involving the solving of some coupled electromagnetic and thermal field problems. For these applications, the electromagnetic field is the heat source, and the boundary conditions change during the hardening process.

The analysis of the electromagnetic field in a sinusoidal quasi-stationary regime in eddy current problems is done starting from the following equation [5]:

$$\nabla \mathrm{x}\mathbf{E} = -\frac{\partial \mathbf{B}}{\partial t};\ \nabla \mathrm{x}\mathbf{H} = \mathbf{J};\ \mathbf{J} = \sigma\mathbf{E} + \mathbf{J_0} \quad (1)$$

In the case of conductive media, $\sigma > 0$ and $\mathbf{J}_0 = 0$, and in insulating media, $\sigma = 0$. The domains with the imposed current density $\mathbf{J}_0$, like coils, are part of the insulating media.

$$\mathbf{B} = \mu\mathbf{H} \quad (2)$$

The constitutive equation **B-H** is non-linear, because the physical properties of the medium depend on temperature. Because of this nonlinearity, the solving of the electromagnetic field problems in the quasi-stationary regime is very difficult. An effective method to solve these problems was proposed by [6], the non-linear medium being replaced by a linear computing medium whose magnetic polarization is corrected according to magnetic induction. (1), (2) represent a system of 4 equations with the unknowns **B**, **H**, **E**, **J**.

By applying the operator ∇x and taking into account the equations (1), (2), we obtain the following equation:

$$\nabla \mathrm{x}\left(\frac{1}{\sigma}\nabla \mathrm{x}\mathbf{H}\right) + \mu\frac{\partial \mathbf{H}}{\partial t} = 0 \quad (3)$$

Equation (3) can be used to determine the electromagnetic field in a domain that is entirely conductive, and whose boundary conditions are imposed for the tangential component of $\mathbf{H_t}$ [7]. If the conductive medium is also homogeneous, $\mathbf{J} = \sigma\mathbf{E}$, σ=ct., μ= ct., we obtain an equation of the form:

$$\nabla x\left(\nabla x\mathbf{E}\right) + \mu\sigma\frac{\partial \mathbf{E}}{\partial t} = 0 \qquad (4)$$

but $\nabla x\left(\nabla x\mathbf{E}\right) = \nabla(\nabla \cdot \mathbf{E}) - \Delta\mathbf{E} = -\Delta\mathbf{E}$

equations (3) and (4) become:

$$-\Delta\mathbf{H} + \mu\sigma\frac{\partial \mathbf{H}}{\partial t} = 0 \qquad (5)$$

$$-\Delta\mathbf{E} + \mu\sigma\frac{\partial \mathbf{E}}{\partial t} = 0 \qquad (6)$$

The determination of the electromagnetic field in the quasi-stationary regime is usually done numerically, a lot of scientific research of specialists in electrical engineering going in this direction [8], [9], [10], [11], [12].

3. THERMAL FIELD ANALYSIS

The thermal field is described by Fourier's equation:

$$-\nabla \cdot (\lambda \nabla \theta) + c_V \frac{\partial \theta}{\partial t} = p \qquad (7)$$

where: λ is the thermal conductivity, c_V is the volumetric thermal capacity of the material, and p is the volume density of the power that converts from the electromagnetic form into heat. The boundary condition is:

$$\lambda\frac{\partial \theta}{\partial n} + \alpha(\theta - \theta_e) = 0 \qquad (8)$$

where: α is the thermal transfer coefficient at the surface, and θ_e is the temperature outside the domain. If α=0, the boundary conditions are homogeneous Neumann-type conditions, and if λ = 0, the boundary conditions are Dirichlet-type conditions.

4. NUMERICAL RESULTS

The numerical analysis of the electromagnetic and thermal field was carried out using the ELTA program. This program provides fast and accurate results on the simulation of electromagnetic and thermal phenomena coupled to induction heating using a single dimension. The program can be used to find optimal correspondence between heating time, temperature, and power. ELTA is a one-dimensional 1D computational program, which can take into account the length of the coil and of the cylindrical workpiece, and these problems are solved using the "Total Flux Method". This method is based on the substitution of the inductor-piece system with a magnetic circuit, providing a preliminary assessment of an induction process or induction heating system [13]. The ELTA program can be used separately or in combination with other 2D or 3D programs. Using ELTA involves 5 steps:

1 – introducing the sizes and material properties of the piece;
2 – defining the inductor: length, number of spirals, the shape of the inductor spiral section, the load adaptation type, and the sizes of the short network;
3 – defining the process: the type of the simulation process (induction heating or the thermal transfer phase), the input values of the inductor-semi product system (voltage, current, power), that can be defined on the generator or inductor, the heating time, the time step and defining the convection and radiation coefficients for heat transfer processes;
4 – the program running phase;
5 – the result phase.

Figure 1 shows the geometry and the sizes of the piece to be simulated using the ELTA program. The piece is made of OLC45, surface hardening is done throughout the length of the piece, and the depth of the hardened layer ranges between 1,4÷1,6 mm.

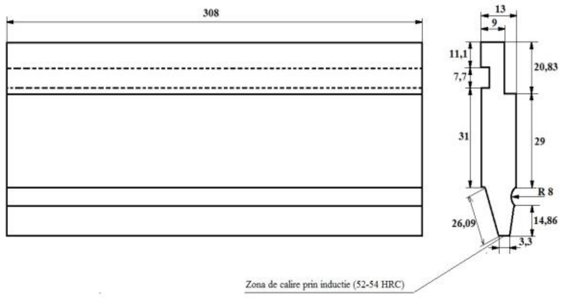

Figure 1. The geometry of the workpiece

The program does not take into account the length of the piece, and calculates the surface hardening process using the feed speed of the piece. The configuration of the hardening system is shown in Figure 2.

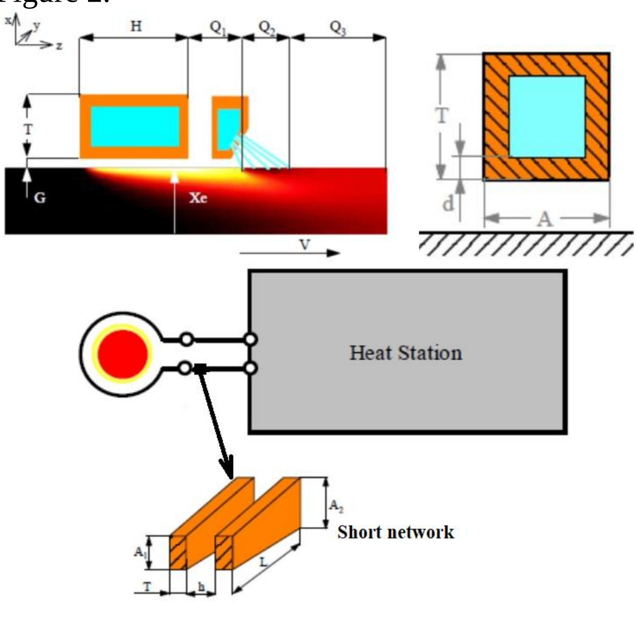

Figure 2. System configuration

Table 1 shows the values of the input quantities for 4 distinct cases studied.

Table 1. Values of the input quantities for cases studied

	f [Hz]	P_{ind} [W]	v_{av} [cm/s]	t_i [s]
Case I	2500	1206,6	0,1	10
Case II	2500	3105,7	0,5	2
Case III	5000	242,45	0,1	10
Case IV	5000	599,75	0,5	2

Case I. Figure 3 presents the temperature variation depending on time and hardening depth, and Figure 4 shows the temperature variation depending on hardening depth and time.

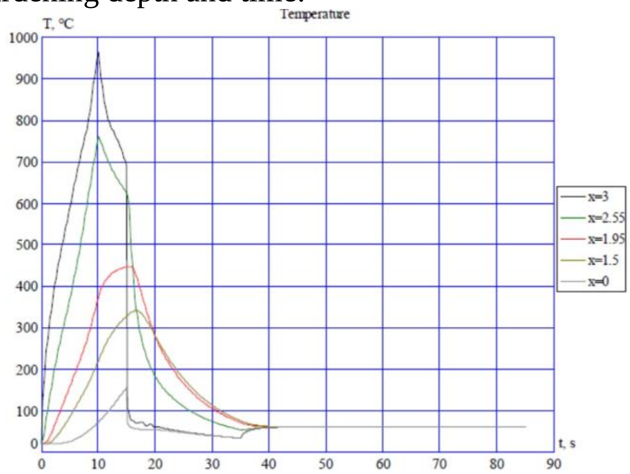

Figure 3. Temperature variation depending on time and hardening depth

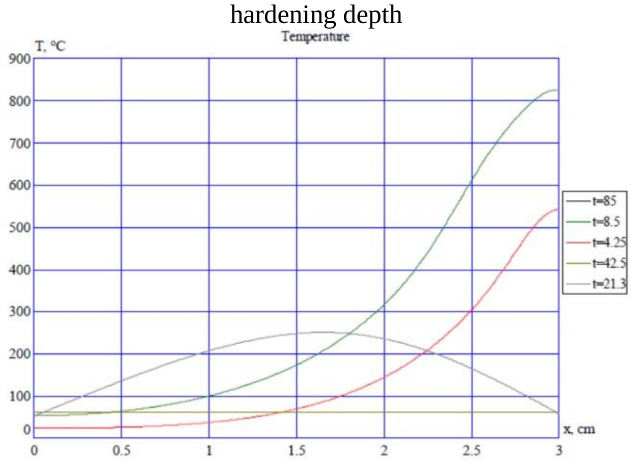

Figure 4. Temperature variation depending on hardening depth and time

The piece needs 10 seconds to reach the optimal hardening temperature of 860 ^{0}C and the hardening depth of 1,6 mm, at a constant speed of movement of v=0,1 cm/s. After 10 seconds, the electrical and power parameters of the model stabilize at optimal values for the hardening process. Figure 5 shows the time variation of specific power on the surface of the piece, and Figure 6 presents the power variation in the hardening system.

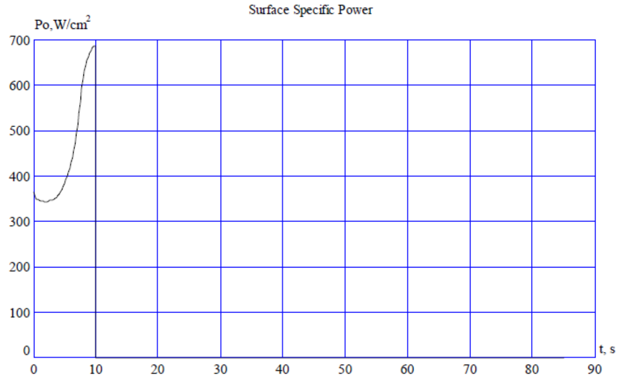

Figure 5. Time variation of specific power on the moving surface

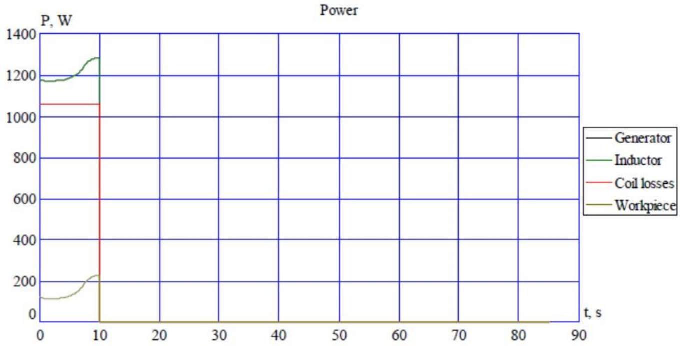

Figure 6. Power variation in the hardening system

Case II. In this case, the frequency is the same as in the first case, the power, the speed of movement, and the hardening time change. Figure 7 shows the temperature variation depending on time and hardening depth, and Figure 8 presents the temperature variation depending on hardening depth and time.

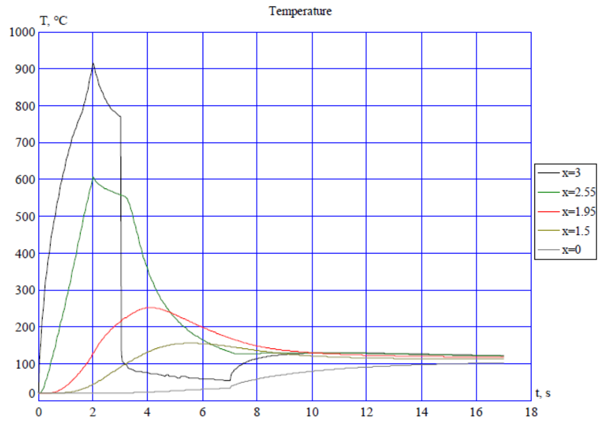

Figure 7. Temperature variation depending on time and hardening depth

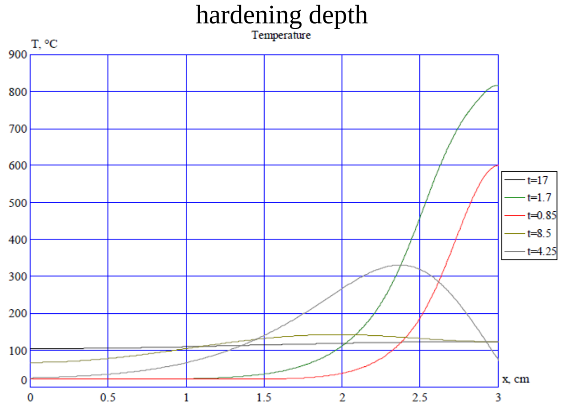

Figure 8. Temperature variation depending on hardening depth and time

The piece needs 2 seconds to reach the optimal hardening temperature of 860 ^{0}C and the hardening depth of 1,6 mm, at a constant speed of movement of v_{av}=0,1 cm/s. If the speed of movement of the piece increases from v_{av}=0,1 cm/s to v_{av}=0,5 cm/s, there is an increase in power, if the power increases, the hardening time decreases.

At the same frequency of 2500 Hz, at an increased speed of movement, the required power increases (Figures 9 and 10). After 2 s, the electrical and energy parameters of the model are stabilized at optimal values.

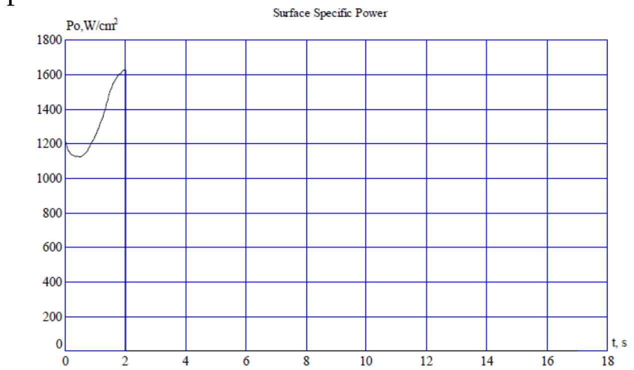

Figure 9. Time variation of specific power on the moving surface

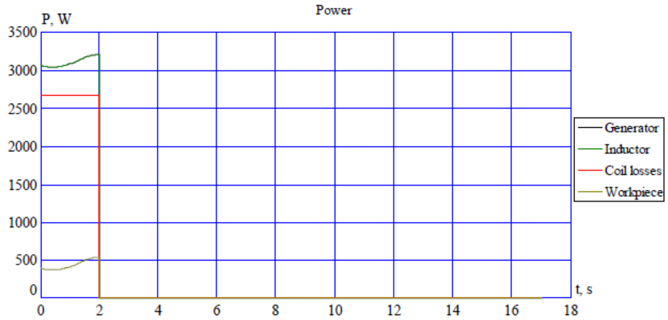

Figure 10. Power variation in the hardening system

Case III. In this case, the frequency is 5000 Hz, the power, the speed of movement, and the hardening time change. Figure 11 shows the temperature variation depending on time and hardening depth, and Figure 12 presents the temperature variation depending on hardening depth and time.

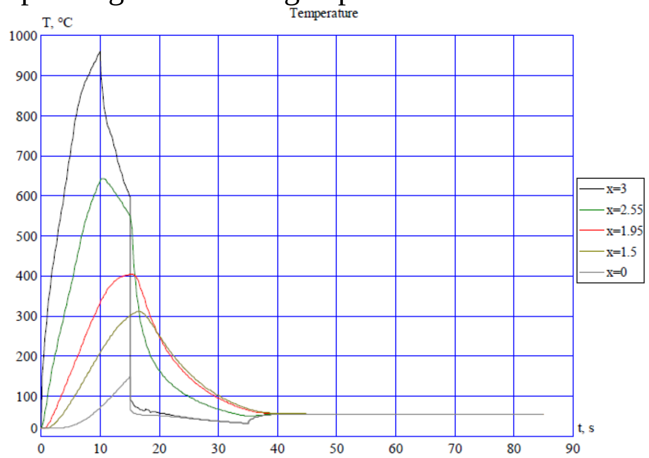

Figure 11. Temperature variation depending on time and hardening depth

The piece needs 10 seconds to reach the optimal hardening temperature of 860 ^{0}C and the hardening depth of 1,6 mm, at a speed of movement of v_{av}=0,5 cm/s. After 10 s, the electrical and energy parameters are stabilized at the optimal values of the hardening process (Figures 13 and 14).

At a constant speed of movement, v_{av}=0,5 cm/s, the hardening depth is constant, at high frequencies, the hardening power decreases.

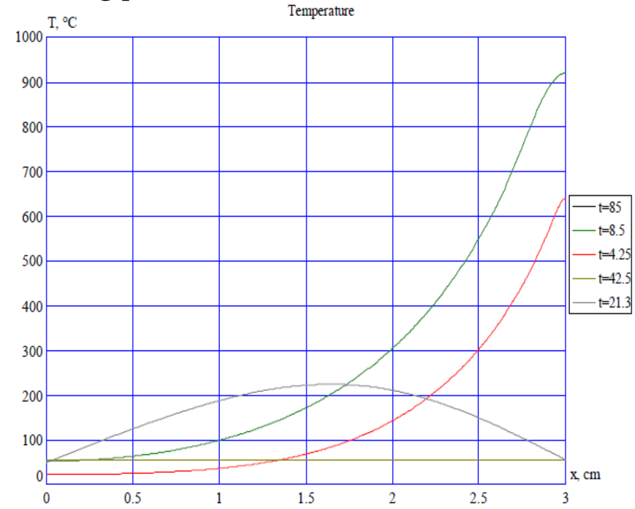

Figure 12. Temperature variation depending on hardening depth and time

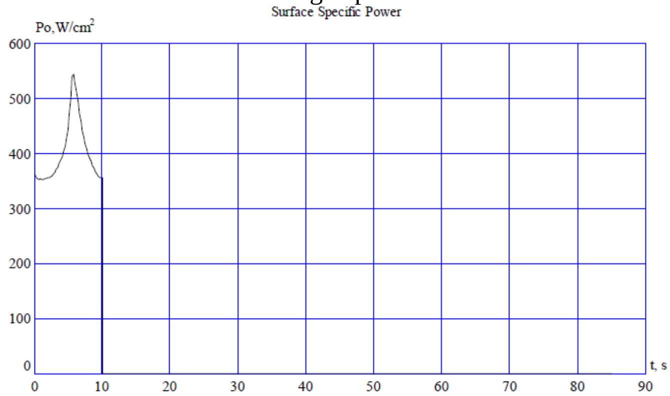

Figure 13. Time variation of specific power on the moving surface

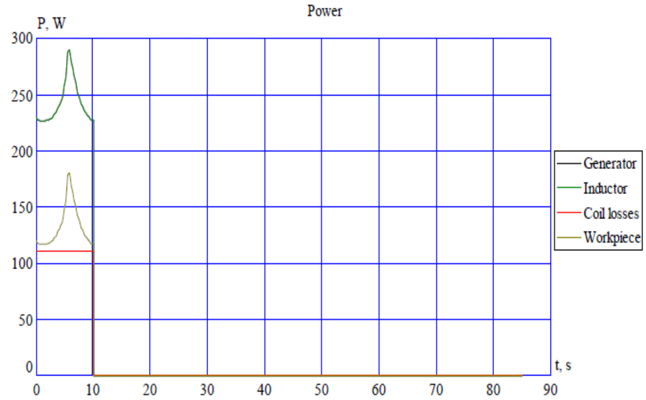

Figure 14. Power variation in the hardening system

Case IV. In this case, the frequency is the same as in case III, only the power, the speed of movement, and the hardening time change. Figure 15 shows the temperature variation depending on time and hardening depth, and Figure 16 presents the temperature variation depending on hardening depth and time.

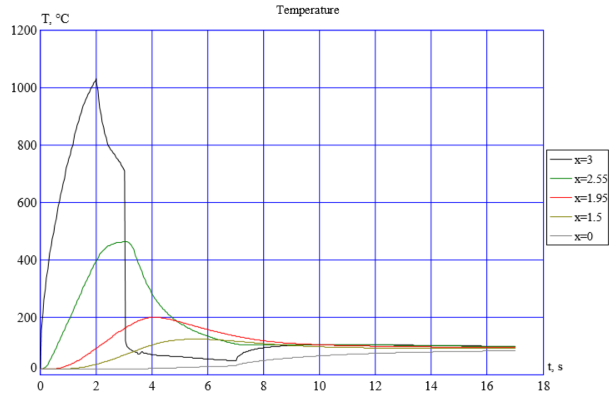

Figure 15. Temperature variation depending on time and hardening depth

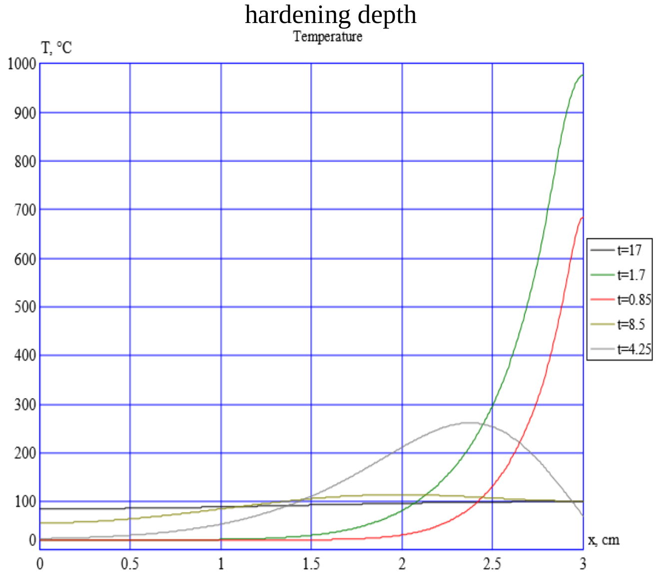

Figure 16. Temperature variation depending on hardening depth and time

The piece needs 10 seconds to reach the optimal hardening temperature of 860 ^{0}C and the hardening depth of 1,6 mm, at a speed of movement of v_{av}=0,1 cm/s. If the speed of movement of the piece increases from v_{av}=0,1 cm/s to v_{av}=0,5 cm/s, there is an increase in power. After 2 s, the electrical and energy parameters are stabilized at the optimal values of the hardening process, as shown in Figures 17 and 18.

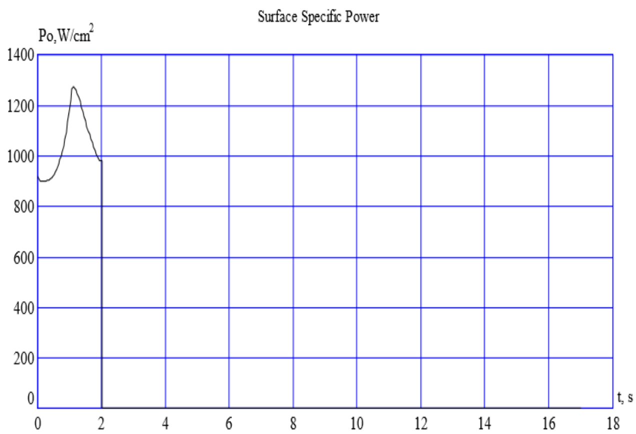

Figure 17. Time variation of specific power on the moving surface

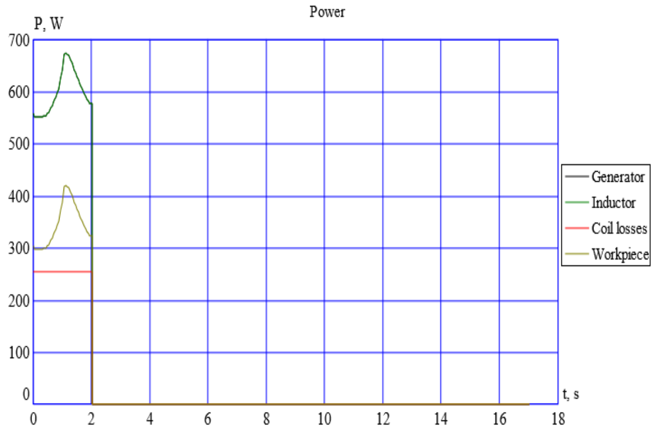

Figure 18. Power variation in the hardening system

5. CONCLUSIONS

In this paper, we performed simulations of the surface hardening of a piece using the ELTA 1 program. By using this program, the optimal correspondence between the heating time, temperature and power was found. If power is greatly increased, very low hardening times are obtained, which cannot be achieved in practice.

The relationship between power, time, temperature, and depth of penetration during the hardening allows the user to modify the characteristics of the induction hardening equipment in order to optimize the process.

Acknowledgement

"This work was supported by a grant of the Romanian Ministry of Research and Innovation CCCDI – UEFISCDI, project number PN-III-P2-2.1-CI-2017-0160, within PNCDI III".

6. REFERENCES

1. Rudnev V., Loveless D., Cook R., Black M., Handbook of Induction Heating, *Marcel Dekker Inc., New York, Basel*, (2003).
2. Lupi S., Modelling for research and industrial development in induction heating, *4th Int. Conf. on EM Processing of Material EPM 2003, Oct. 14-17, LyonFrance*, (2003).
3. Demidovitch V., Skvortsov V., Optimisation of Induction Heating Devices: *Experiece of the Last 20 Years, HIS 98, Padova, Italia* (1998).
4. Buidoş, Tr., Maghiar, T., Soproni, D., Pantea, M. Some aspects regarding inductive heating application in order to make the magnetron device, *PIERS - Progress in Electromagnetics Research Symposium*, Pisa; Italy, pp. 535-538 (2004).
5. Hănţilă F., Preda G., Vasiliu M., Leuca T., Della Giacomo E., Calculul numeric al curentilor turbionari. *Editura ICPE*, (2001).

6. Ciric I. R. and Hantila F. I., An efficient harmonic method for solving nonlinear time-periodic eddy-current problems, *IEEE Trans. Magn*, vol. 43, no.4, pp.1185-1188, (2007).
7. Hănţilă F., Preda G., Vasiliu M., Leuca T., Della Giacomo E., Calculul numeric al curentilor turbionari, *Editura ICPE*, (2001).
8. Ciric I. R., Hanţilă F. I., Maricaru M., Novel Solution to Eddy-Current Heating of Ferromagnetic Bodies With Nonlinear B-H Characteristic Dependent on Temperature, *IEEE Trans. on Magn,* Vol. 44, No. 6, pp. 1190-1193, (2008).
9. Ciric I. R., Hănţilă F. I., Maricaru M., Marinescu S., Efficient Analysis of the Solidification of Moving Ferromagnetic Bodies With Eddy-Current Control, *IEEE Trans. on Magn.* Vol. 45, No. 3, pp. 1238-1241, (2009).
10. Hănţilă I. F., Ciric I. R., Maricaru M., Vărăticeanu B., Bandici Livia, A dynamic overrelaxation procedure for solving nonlinear periodic field problems, *Revue Roumaine des Sciences Techniques serie Electrotechnique et Energetique*, Bucureşti., Vol. 56, No.2, pp. 169-178, (2011).
11. Burca A., Trip N.D., Leuca T., Considerations on the Design of a Low Power Induction Heating System, *International Symposium on Fundamentals of Electrical Engineering,* București, Nov. 28-29, (2014).
12. Maricaru M., Codrean M., Leuca T., Bandici Livia, Vasilescu G. M., Thermal Treatment of Ferromagnetic Bars, *Revue Roumaine des Sciences Techniques serie Electrotechnique et Energetique,* Bucureşti, Year: 2017, Tome: 62, Issue: 3, pp. 225-228, (2017).
13. Nemkov V.S., Role of Computer Simulation in Induction Heating Techniques. *International Induction Heating Seminar, May 13-15,* Padua, Italy, pp.301 – 309, (1998).